



Parametric studies using finite element modeling for the evaluation of the performance of tiered MSE walls under seismic loading

Ananya Srivastava¹ · Vinay Bhushan Chauhan¹

Received: 29 January 2021 / Accepted: 4 May 2021 / Published online: 11 June 2021
© Springer Nature Switzerland AG 2021

Abstract

Whenever a need arises to construct a high retaining wall, the construction of a mechanically stabilized earth (MSE) retaining wall in a multi-tiered configuration is a viable approach than the construction of a single-tiered (rectangular wall). However, the behavior of multi-tiered MSE walls is complex, and unfortunately, the behavior of such walls under seismic loading has not yet been entirely investigated. Therefore, this study performs an exhaustive comparative analysis, on multi-tiered and rectangular MSE walls through a finite element method-based numerical computational tool to look into its performance under seismic loading and their potential failure envelope, i.e., wedge angle. Additionally, this study investigates the influence of the parameters such as the number of tiers, offset distance (D), and horizontal seismic acceleration coefficient (k_h) on the walls. The potential failure envelopes of the various wall models are explored, which indicate a combination of overturning and sliding failure accompanied by a distortion of the leveling pad of the walls. However, the sliding behavior reduces as the k_h increases and the overturning failure is more prominent. This study proposes a wedge angle correction factor (C_Θ) to normalize the deviation of the angle of the potential failure plane under seismic loading, based on the assumption that the standard value of the potential failure plane defined by Federal Highway Administration (FHWA) is valid for all multi-tiered walls since none of the design manuals have suggested clear guidelines that can demonstrate the formation and progression of the wedge angle under seismic loading conditions for multi-tiered walls. The factor of safety (FOS) of the various wall models simulated in the present study satisfies the FHWA guidelines, thus suggesting the construction of tiered walls, at places where huge excavation required for the construction of a rectangular wall is impractical. In the numerical simulations, where the FOS obtained is unsatisfactory as per FHWA guidelines, the current study suggests increasing the length of reinforcement and/or decreasing the vertical spacing between the reinforcing layers to enhance the overall stability of such walls.

Keywords Multi-tiered wall · MSE retaining wall · Critical wedge angle · FEM · Strength reduction method

List of symbols

L	Length of the reinforcement layer (m)	v	Vertical spacing between the two reinforcing layers (m)
FOS	Factor of safety	ϕ	Angle of internal friction of soil (degrees)
D	Offset distance between the two consecutive tiers of the tiered wall system (m)	β	Critical wedge angle
H_1	Height of the lowermost wall (m)	β^*	Critical wedge angle suggested by FHWA
H_2	Height of the middle wall (m)	k_h	Horizontal seismic acceleration coefficient
H_3	Height of the topmost wall (m)	R_{int}	Interface coefficient
		C_Θ	Wedge angle correction factor

✉ Vinay Bhushan Chauhan
vbcce@mmmut.ac.in; chauhan.vinaybhushan@gmail.com

Ananya Srivastava
ananyashri.work@gmail.com

¹ Civil Engineering Department, Madan Mohan Malaviya University of Technology, Gorakhpur, Uttar Pradesh 273010, India

Introduction

The accelerated necessity for the futuristic and visionary construction technology, to contest the numerous innovative upcoming challenges while erecting high-rise, heavy engineering infrastructures such as dams, embankments, and retaining walls, has uncovered the incompetency and

obsolescence of the conventional methods of earth mass retention. The conventional gravity or cantilever walls require a bulky cross section to withstand the horizontal thrust exerted on the wall in case of high retention of the earth mass. To minimize the horizontal thrust on such stiff retaining walls, mechanically stabilized earth retaining walls are constructed, which are reinforced with polystyrene geofoam, geonets, geosynthetics, knitted geotextiles, galvanized steel strips, geocomposites, etc. [1–4].

A mechanically stabilized earth (MSE) wall is a compound structure comprising alternate layers of compacted backfill and embedded soil reinforcements, attached to a wall facing. The addition of reinforcements in the soil improves the engineering properties of the soil mass and provides substantial tensile strength, thus increasing the load-bearing capacity of the structure [5]. These walls can accommodate high differential settlement without distress and also can withstand extreme loads (bridge abutment footings, cranes) and have a high resistance to seismic and other accidental forces. They also perform the primary function of preventing erosion of the backfill material, resulting in a coherent gravity structure that is flexible and can carry a variety of heavy loads [6].

The design and construction of tall MSE walls have escalated owing to their unmatched performance, improved qualitative index, and serviceability. As a result of their superior geometry, bigger wall heights can be achieved for critical applications in earthquake-prone areas as well [7]. The increased restrictions of wetlands, right of way, and other space restraining conditions have also contributed to their growing familiarity and acceptance among designers and engineers [8, 9]. For instance, MSE walls have been built in many cities around the world such as Florida, Georgia, Pennsylvania, California, New York, and Texas covering more than 850,000 m² of landmass. These walls include a rectangular, two-tiered, and multi-tiered construction pattern. Few examples of the aforementioned walls comprise a four-tiered wall system in the USA 290 in Austin, Texas, a two-tiered wall system in the USA 375 at the Socorro Bridge, a Hybrid Soil–Nail MSE Wall for St Jacques–Pullman Walls, Montreal, Quebec, and a tiered MSE wall constructed in Kanaka Durga temple in Vijayawada, India [10–12].

Often, the favorable geographical and topographical conditions required for the construction of tall MSE walls are hard to achieve. Moreover, for a high MSE retaining wall, tensile stresses in the reinforcing layers situated at the bottom quarter of the wall are very high. Under such circumstances, the construction of MSE walls in a tiered configuration is preferred as it eradicates the requirement of high tensile reinforcement to be placed at the bottom quarter of the walls.

As suggested by FHWA [13], when there arises a need to construct tall walls, preference must be given to the wall

construction in a tiered manner. The reconfiguration of a tall wall in the form of superimposed shorter walls reaching similar height provides a fresh beginning with a new leveling pad. It offers reduced vertical stresses on the rigid facing elements and allows better control of the vertical alignment of the wall facing. Analytically, the offset distance between the superimposed walls renders another beneficial effect as an equivalent sloped face of the wall leads to lesser lateral forces on the whole wall system.

From the available literature on MSE retaining walls, which is attained by continuous exhaustive experimental procedures, field study, analytical derivations, and numerical simulations, it is evident that multi-tiered walls render a better outcome in comparison with rectangular tall walls, especially when it is necessary to erect a high-rise MSE retaining wall which is competent in terms of stability, fiscal concerns, and visual appeal. The findings from limited studies on multi-tiered reinforced soil walls using numerical simulations clearly show that the performance of a tall MSE wall can be significantly improved by constructing it in a tiered fashion [14–17].

The design and analysis of tiered MSE walls are usually more complex than the conservative MSE retaining walls due to their compounded geometrical configuration whose limited guidelines can be found in AASHTO, FHWA, and NCMA design manual [13, 18, 19]. In contrast to the conventional MSE walls, the reinforcing parameters (vertical spacing, length, and offset distance) for tiered walls cannot be estimated by applying available design calculations [20]. The performance analysis of the multi-tiered MSE retaining walls is multifaceted, and regrettably, available previous studies are not sufficient for a satisfactory examination of multi-tiered walls and their behavior under seismic loading conditions.

Hence, the objective of this study is to examine the stability of multi-tiered MSE walls using finite element-based strength reduction method and investigate its behavior by quantifying the effects of reinforcement length (L), offset distance (D), and the number of tiers of the wall under seismic loading. Also, in the prior studies, both sophisticated and general constitutive models for geosynthetic reinforcements and soils have been engaged to mathematically analyze the performance of multi-tiered geosynthetic reinforced earth retaining walls [21]. Furthermore, this study also evaluates the potential failure planes for all the walls since it provides an insight into the possible mode of wall distortion. Furthermore, the strength reduction factor for all walls is also evaluated which in turn provides the FOS of the wall systems. The FOS aids in improving the understanding regarding the improved design of such walls when constructed in a tiered fashion. Hence, the scope of this study is to incorporate the various force transfer mechanisms in tiered MSE retaining walls, the complex interactions between the backfill and the

reinforcing elements, and the interaction between the backfill and the facing panels to examine the outcomes obtained from the numerical simulation of such walls.

Numerical modeling

The numerical analysis in the current study is carried out using a computational tool OPTUM G2 [22], an FEM-based program dedicated to geotechnical deformation and stability analysis under plane strain conditions. A two-dimensional prototype is considered for the regeneration of the MSE walls in rectangular and tiered fashion both 18 m high, modeled under three different conditions as, an 18-m-high single-tiered wall (T_1), a tiered wall system having two tiers each 9 m high (T_2), and another tiered wall system having three tiers each 6 m high (T_3).

Each of the tiered wall systems has further been categorized and configured based on the three offset distances (D) between the consecutive tiers, D_1 , D_2 , and D_3 , where $D_1 = 0.9$ m, $D_2 = 4.0$ m, and $D_3 = 6.0$ m. The variation in the offset distances significantly affects the behavior of the tiered MSE walls. These various offset distances are calculated to examine the difference in the wall behavior thoroughly.

The horizontal seismic acceleration coefficient (k_h) is varied at 0, 0.12, 0.24, and 0.36 in the present study. The wall heights (H_1 , H_2 , and H_3), reinforcement lengths (L_1 , L_2 , and L_3), and offset distances (D_1 , D_2 , and D_3) between the walls for a tiered superimposed wall are described in Figs. 1, 2, and 3.

Reinforcement lengths and offset distances for different tiers considered in this study as per FHWA [13] are summarized in Tables 1 and 2.

When the offset distance is small, there is an overlapping of the reinforcements such that the interaction of two walls occurs, and full active thrust is mobilized. On the other hand, in the case of large offset distance, no overlapping of the reinforcements takes place and each wall behaves independently and can be designed individually [23]. Hence, no active earth pressure acts from the backfill, which needs to be taken into account during external stability calculations. The upper tiers, in the tiered MSE retaining wall, can be considered as a corresponding surcharge whose magnitude relies on the offset distance, and its extent is calculated conferring to the offset distance as stated in NCMA [19]. If the offset distance is small, the wall behaves as a single entity, and if the tiers lie far away, each tier behaves independently and imparts no effect over the other. As it is evident that the offset distance plays a major role in the behavior of such walls, consideration of all possible cases (three cases, as mentioned earlier) of offset distances is taken into account.

In the present numerical model, the geosynthetic reinforcement is demonstrated as an elastic material that can endure the tensile load [24]. An elastoplastic model is taken to simulate the backfill following the Mohr–Coulomb failure criterion as the Mohr–Coulomb failure criterion is widely used for geotechnical applications, and indeed, a large number of the routine design calculations in the geotechnical area are still performed using the Mohr–Coulomb criterion. Modeling the interfaces within the reinforced soil walls has always been an essential task to predict the behavior of such walls precisely. In the current study, interface elements are assigned at three different locations, viz. at the interface of reinforcements–facing panels, soil–geosynthetic reinforcement, and soil–facing panels [25, 26]. The roughness of the interaction was

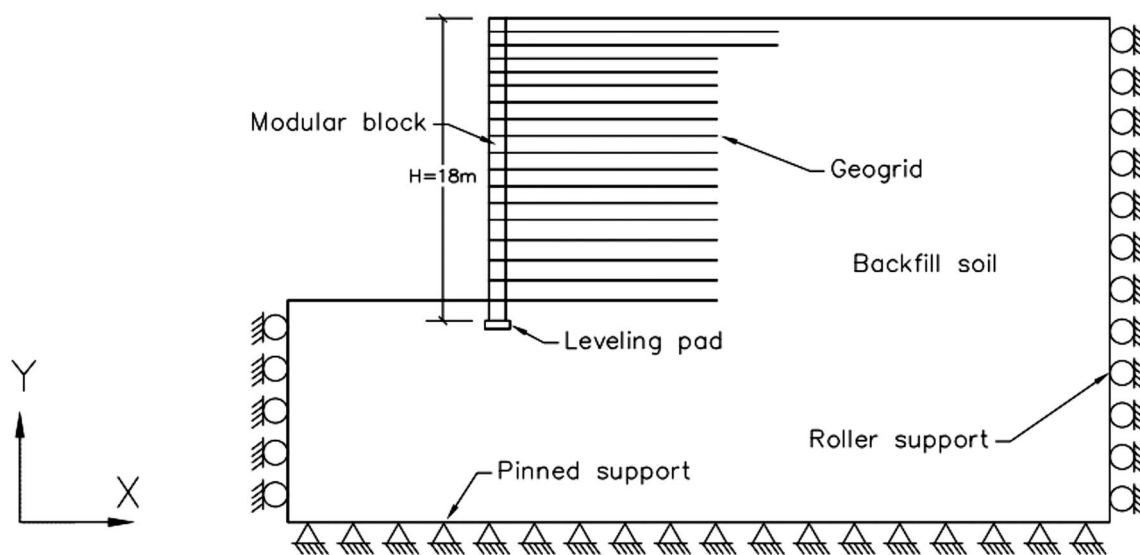


Fig. 1 Geometrical configuration of the 18 m high rectangular MSE wall modeled in the present study

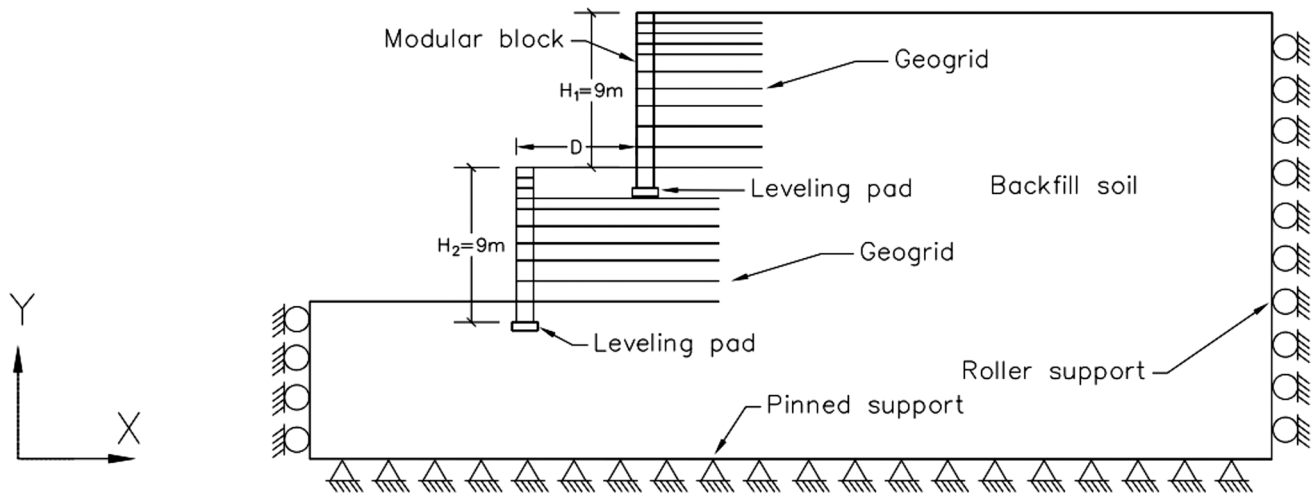


Fig. 2 Geometrical configuration of the 18 m high two-tiered MSE wall modeled in the present study

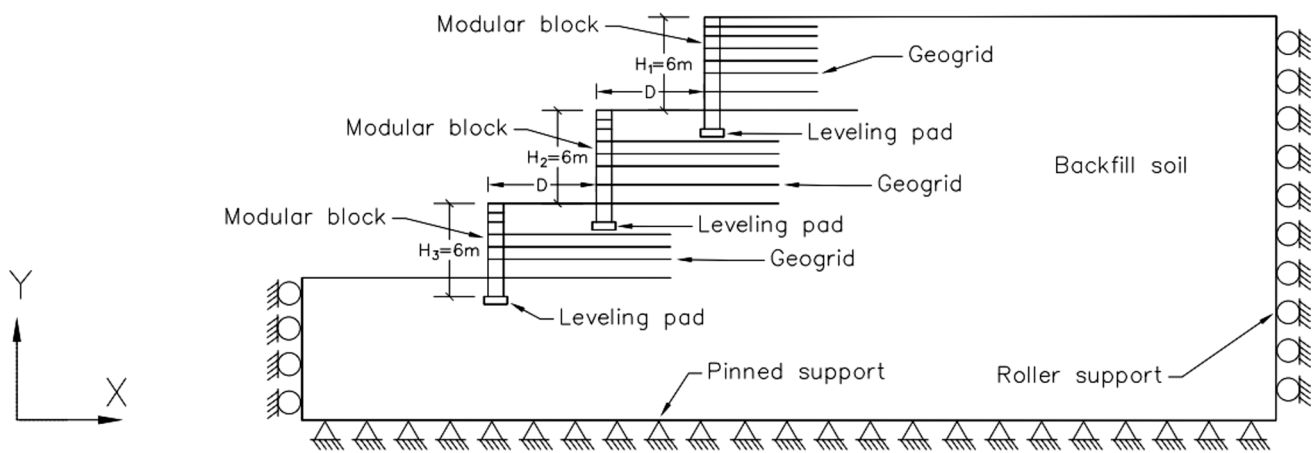


Fig. 3 Geometrical configuration of the 18 m high three-tiered MSE wall modeled in the present study

Table 1 Reinforcement lengths considered in static analysis for different tiers as per FHWA [13]

Wall	Height	Static analysis (length of reinforcement)	Wall description
T ₁	18 m	L = 0.9H = 16.2 m L = 0.7H = 12.6 m	For the first two layers For other layers
T ₂ D ₁ , T ₂ D ₂ , T ₂ D ₃	H ₁ = H ₂ = 9 m	L ₁ = 0.7H ₁ = 4.2 m L ₂ = 0.6H = 10.8 m	
T ₃ D ₁ , T ₃ D ₂ , T ₃ D ₃	H ₁ = H ₂ = H ₃ = 6 m	L ₁ = 0.7H ₁ = 4.2 m L ₂ = 0.6H = 10.8 m	

H₁ = height of the upper-tier, H₂ = H₃ = height of the lower tier, H = total height of the wall

established by selecting an appropriate value of the interface coefficients, R_{int} at all the positions of the interfaces. The interface coefficient values of 0.7, 0.8, and 0.8 have been assigned in the MSE walls for the soil–geosynthetic interface, concrete facing panel–geosynthetic interface, and soil–facing panels, respectively [27].

To provide apt boundary conditions for the reinforced soil wall system, the bottom boundary of the model is kept fixed and roller supports are provided at the vertical boundaries of the mesh [28]. For maintaining the accuracy of results obtained from the numerical simulations, a suitable number of elements are provided in the mesh [29, 30]. To achieve a

Table 2 Reinforcement lengths considered in the seismic analysis for different tiers as per FHWA [13]

Wall details	Reinforcement configuration	Wall description
T ₁	L = 1.1H = 19.8 m L = 0.9H = 16.2 m	For the first two layers For other layers
T ₂ D _{1_0.12} , T ₂ D _{1_0.24} , T ₂ D _{1_0.36} T ₂ D _{2_0.12} , T ₂ D _{2_0.24} , T ₂ D _{2_0.36} T ₂ D _{3_0.12} , T ₂ D _{3_0.24} , T ₂ D _{3_0.36}	L ₁ = 1.0H ₁ = 9 m L ₂ = 1.0H = 18 m	
T ₃ D _{1_0.12} , T ₃ D _{1_0.24} , T ₃ D _{1_0.36} T ₃ D _{2_0.12} , T ₃ D _{2_0.24} , T ₃ D _{2_0.36} T ₃ D _{3_0.12} , T ₃ D _{3_0.24} , T ₃ D _{3_0.36}	L ₁ = 1.0H ₁ = 6 m L ₂ = 1.0H = 18 m L ₃ = 1.0H = 18 m	

H₁ = height of the upper-tier, H₂ = H₃ = height of the lower tier, H = total height of the wall

satisfactory level of the accuracy of the obtained results, a sensitivity analysis is performed by varying the number of elements from 5000 to 20,000. It is found that while keeping the number of elements above 10,000 for the considered mesh, the results do not vary considerably, thus establishing an optimum number of elements to be 10,000 for the wall models used in the current study [31, 32].

The FOS of the MSE wall models is evaluated by using the strength reduction method (SRM). In the strength reduction method, only the strength of the soil mass is reduced while calculating the FOS during various iterations of the analysis process. The results demonstrate that the FOS values of the walls converge after a few iterations. The reduction in strength has diverse impacts on the FOS depending upon the properties of the soil, facing, and the reinforcements [33].

Results and discussion

The significant results of this study are discussed in the following section. This section of the current study deals with the development of the wedge angle, the progression of the displacement vectors, failure planes, and the effect of the horizontal seismic acceleration coefficient and offset distance on the performance of the tiered wall systems.

Critical wedge angle in the tiered wall system

This study incorporates a Mohr–Coulomb model in which for a given retaining wall, the potential failure plane is assumed to be inclined at angle of $45^\circ + \phi/2$ with respect to the horizontal which coincides with the locus of maximum reinforcement tension [13]. Figure 4 illustrates the position of critical wedge angle in a two-tiered wall system where the offset distance (*D*) satisfies the following condition:

$$H_2 \tan \left(45^\circ + \frac{\phi}{2} \right) < D \leq H_2 \tan (90^\circ + \phi). \tag{1}$$

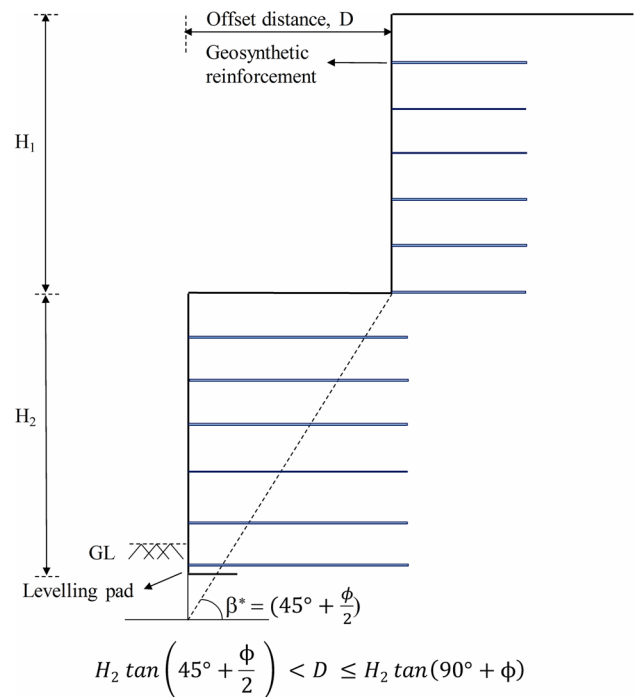


Fig. 4 Position of the critical wedge angle (β^*) for two-tiered MSE wall as suggested by FHWA under static loading conditions [13]

This condition is satisfied at offset distance $D_3 = 6$ m in the present study. Here, it is worth mentioning that the guidelines suggested by FHWA [13] do not discuss the progression of critical wedge angle (β) for walls having more than two tiers or MSE walls under static or seismic loading.

Figures 5, 6, and 7 illustrate the critical wedge angle (β) obtained for various wall models simulated in the present study.

These results highlight the fact that the critical wedge angle decreases with an increase in the magnitude of k_h . The increase in the k_h causes a declination in the stability of the wall system, leading to a failure having lesser tolerance to seismicity. For the rectangular MSE wall, with an increase in k_h from 0 to 0.36, a reduction of 25.4% in β is observed.

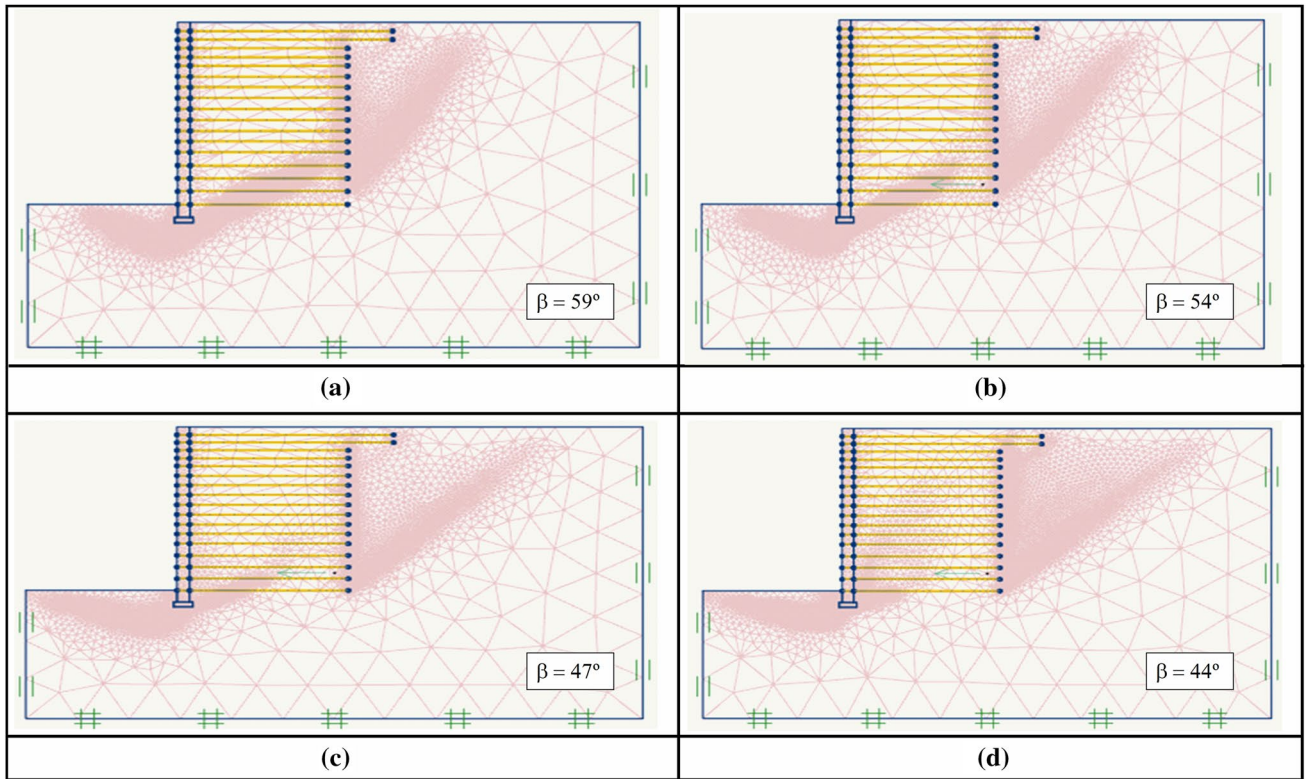


Fig. 5 Critical wedge angle (β) obtained for rectangular MSE wall at **a** $k_h=0$; **b** $k_h=0.12$; **c** $k_h=0.24$; and **d** $k_h=0.36$

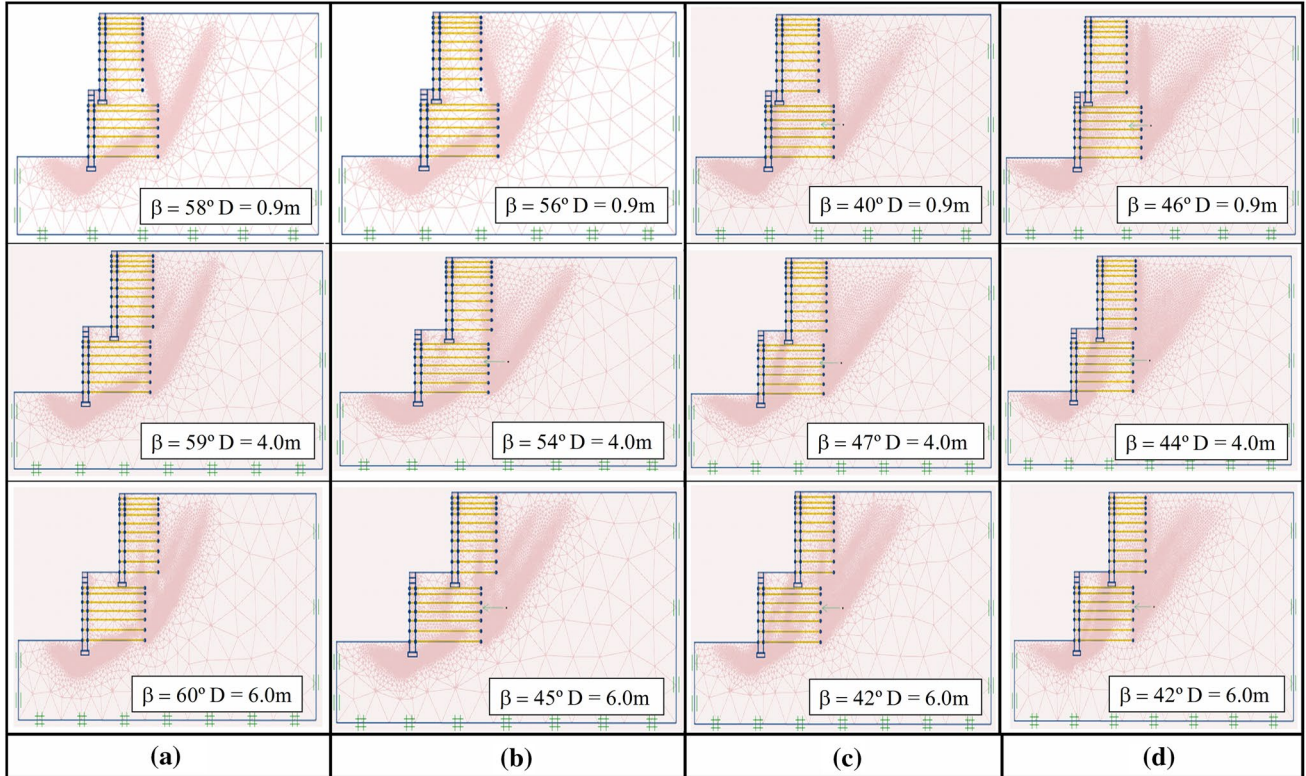


Fig. 6 Critical wedge angle (β) obtained for two-tiered MSE wall at **a** $k_h=0$; **b** $k_h=0.12$; **c** $k_h=0.24$; and **d** $k_h=0.36$

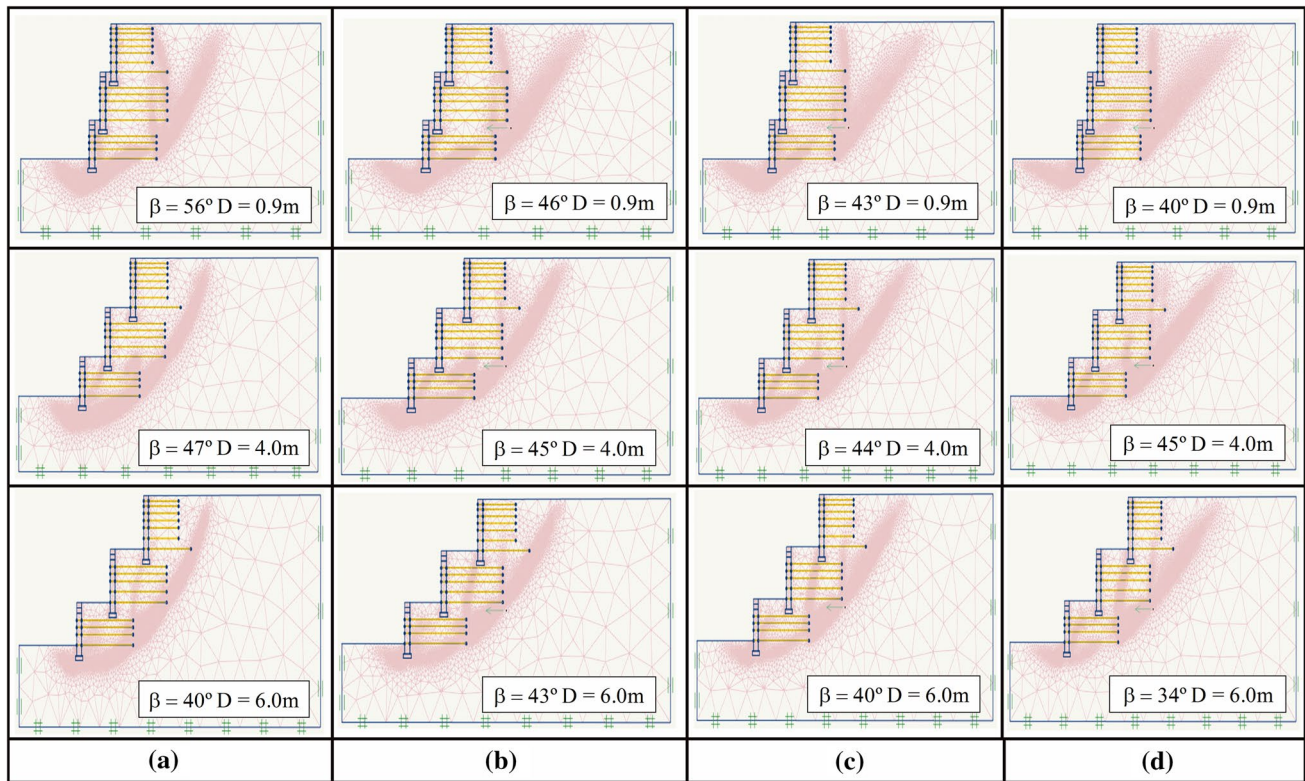


Fig. 7 Critical wedge angle (β) obtained for three-tiered MSE wall at **a** $k_h=0$; **b** $k_h=0.12$; **c** $k_h=0.24$; and **d** $k_h=0.36$

Similarly, for two-tiered walls by varying the k_h from 0 to 0.36 at $D=0.9, 4.0,$ and 6.0 the declination in β is 20.6%, 25.4%, and 30%, respectively. It is also worth noticing here that an increase in the D has caused an increased declination in the β values, thus implying that the β also gets affected with the change in the offset distance of the wall.

For the three-tiered walls, on varying the k_h from 0 to 0.36 at $D=0.9\text{ m}, 4.0\text{ m},$ and 6.0 m , the declination in the β is 28.5%, 4.2%, and 15.0%, respectively. Here, for three-tiered walls, the assumption of decrement of β w.r.t increasing D is not justified since β of T_3D_2 is lesser than β of T_3D_3 . The critical wedge angle β obtained in the present study for the rectangular wall at $k_h=0, 0.12, 0.24,$ and 0.36 is $59^\circ, 54^\circ, 47^\circ,$ and 44° , respectively, and β for two-tiered walls at $D_3 = 6\text{ m}$ and $k_h=0, 0.12, 0.24,$ and 0.36 is $62^\circ, 55^\circ, 42^\circ,$ and 42° , respectively. The critical wedge angle under static loading recommended by the FHWA, β^* [13], equals 62° which is exactly equal to the β obtained in the current study under static loading. The similarity in the results validates the numerical model simulated in this study.

All the values of the β noted from the simulations of all studied models of the MSE wall are summarized in Table 3. Furthermore, a wedge angle correction factor (C_Θ) is introduced to show the variation of β obtained for all wall models with the recommended β^* based on FHWA [13]. This wedge angle correction factor C_Θ is defined as the ratio of

the critical wedge angle based on FHWA [13], β^* and the critical wedge angle obtained for the rectangular and tiered MSE walls under static as well as seismic loading, β . The numerical range of C_Θ for various walls under seismic loading is summarized in Table 3 and is between 1.0 and 1.90. Both β and C_Θ are inversely proportional to each other. A higher β value causes a lower C_Θ , and a smaller β value results in a higher C_Θ .

It is also observed that the variation of the horizontal seismic acceleration coefficient (k_h) affects the potential failure wedge (β) of the walls significantly. Figure 8 denotes a graphical representation of the variation of wedge angle (β) w.r.t the horizontal seismic acceleration coefficient (k_h).

As the k_h increases, β decreases, in turn increasing the correction factor. The rectangular wall shows a reduction of β by 25.4% when the k_h is raised from 0 to 0.36. For the walls $T_2D_1, T_2D_2,$ and T_2D_3 , the β decreases by 26.1%, 28.7%, and 30%, respectively, whereas for $T_3D_1, T_3D_2,$ and T_3D_3 , the β decreases by 28.6%, 4.2%, and 15%, respectively, when the k_h is raised from 0 to 0.36 of the wall systems. Although for the walls T_2D_3 and T_3D_3 , the above deduction fails to lead to a conclusion that D_3 influences the behavior of the wall system and a farther offset distance causes the walls to behave independently from each other. Also, the offset distance (D) affects the β of the tiered walls significantly. It is noticed from Table 3 that on increasing the offset distance,

Table 3 Critical wedge angles β , β^* and wedge angle correction factor (C_Θ) obtained for various wall models simulated in the present study

Wall description	Wedge angle (β) (obtained in the present study)	Wedge angle (β^*) (FHWA) [13] ($45^\circ + \frac{\phi}{2}$)	Wedge angle correction factor, $C_\Theta = \beta^*/\beta$
T ₁ , $k_h = 0.0$	59°	62°	1.05
T ₁ , $k_h = 0.12$	54°	62°	1.14
T ₁ , $k_h = 0.24$	47°	62°	1.31
T ₁ , $k_h = 0.36$	44°	62°	1.40
T ₂ D ₁ _0.0	56°	62°	1.06
T ₂ D ₁ _0.12	56°	62°	1.10
T ₂ D ₁ _0.24	46°	62°	1.24
T ₂ D ₁ _0.36	46°	62°	1.34
T ₂ D ₂ _0.0	56°	62°	0.93
T ₂ D ₂ _0.12	47°	62°	1.16
T ₂ D ₂ _0.24	45°	62°	1.34
T ₂ D ₂ _0.36	46°	62°	1.31
T ₂ D ₃ _0.0	51°	62°	1.03
T ₂ D ₃ _0.12	42°	62°	1.12
T ₂ D ₃ _0.24	43°	62°	1.47
T ₂ D ₃ _0.36	42°	62°	1.47
T ₃ D ₁ _0.0	55°	62°	1.10
T ₃ D ₁ _0.12	46°	62°	1.34
T ₃ D ₁ _0.24	40°	62°	1.44
T ₃ D ₁ _0.36	40°	62°	1.55
T ₃ D ₂ _0.0	44°	62°	1.31
T ₃ D ₂ _0.12	38°	62°	1.37
T ₃ D ₂ _0.24	38°	62°	1.40
T ₃ D ₂ _0.36	42°	62°	1.37
T ₃ D ₃ _0.0	36°	62°	1.55
T ₃ D ₃ _0.12	38°	62°	1.44
T ₃ D ₃ _0.24	32°	62°	1.55
T ₃ D ₃ _0.36	33°	62°	1.82

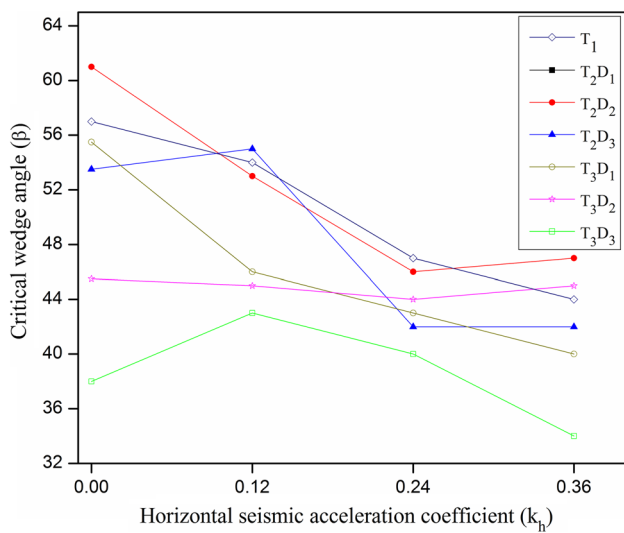


Fig. 8 Variation of the critical wedge angle (β) w.r.t the horizontal seismic acceleration coefficient k_h for all MSE walls studies in the present study

the β of the tiered walls decreases significantly. This might be attributed to the fact that as the offset distance increases, the effect of the surcharge of the walls above each other is reduced, in turn reducing the wedge angle (β).

Potential failure modes of the walls

For the appropriate and sustainable design of any geotechnical structure, understanding of the potential failure modes of such structure is a prime requirement. In view of the above, the potential failure modes of the multi-tiered and rectangular walls under static and seismic loading conditions are evaluated in the present study and shown in Figs. 9, 10, and 11.

From a extensive comparison of all the potential failure modes of walls obtained from the simulation, it is evident that the rectangular wall experiences overturning failure combined with a slight sliding failure as the base of the wall gets displaced minorly, but the upper structure upturns onto the left, disrupting the wall geometry as illustrated in Fig. 9.

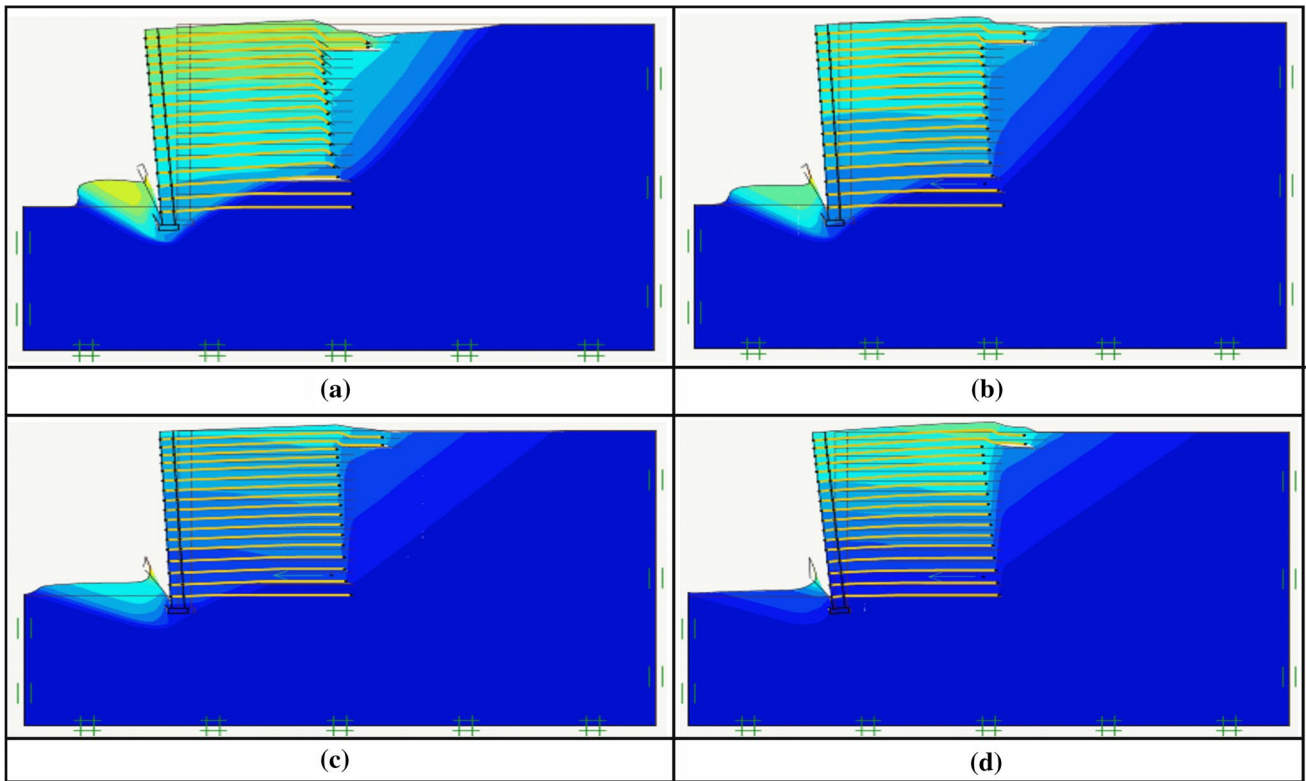


Fig. 9 The mode of failure for rectangular MSE wall at **a** $k_h = 0$; **b** $k_h = 0.12$; **c** $k_h = 0.24$; and **d** $k_h = 0.36$

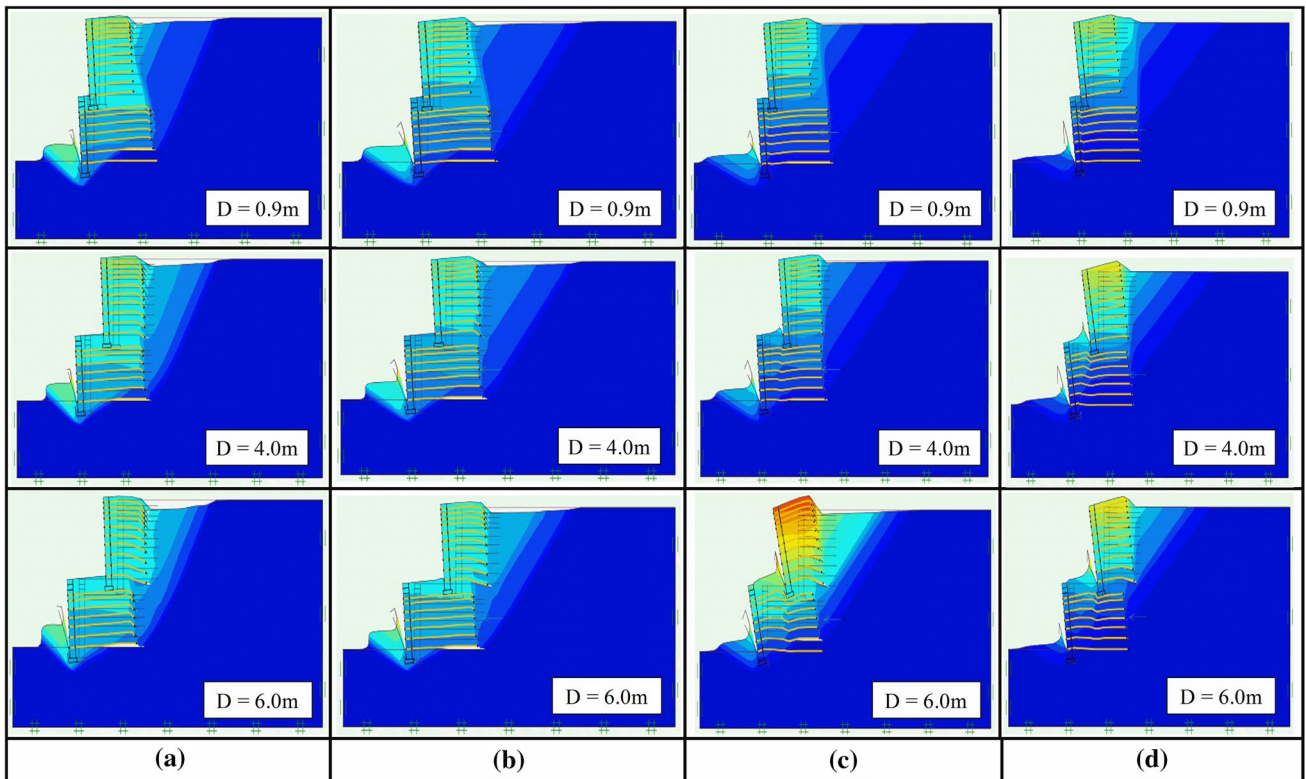


Fig. 10 The mode of failure for two-tiered MSE wall at **a** $k_h = 0$; **b** $k_h = 0.12$; **c** $k_h = 0.24$; and **d** $k_h = 0.36$

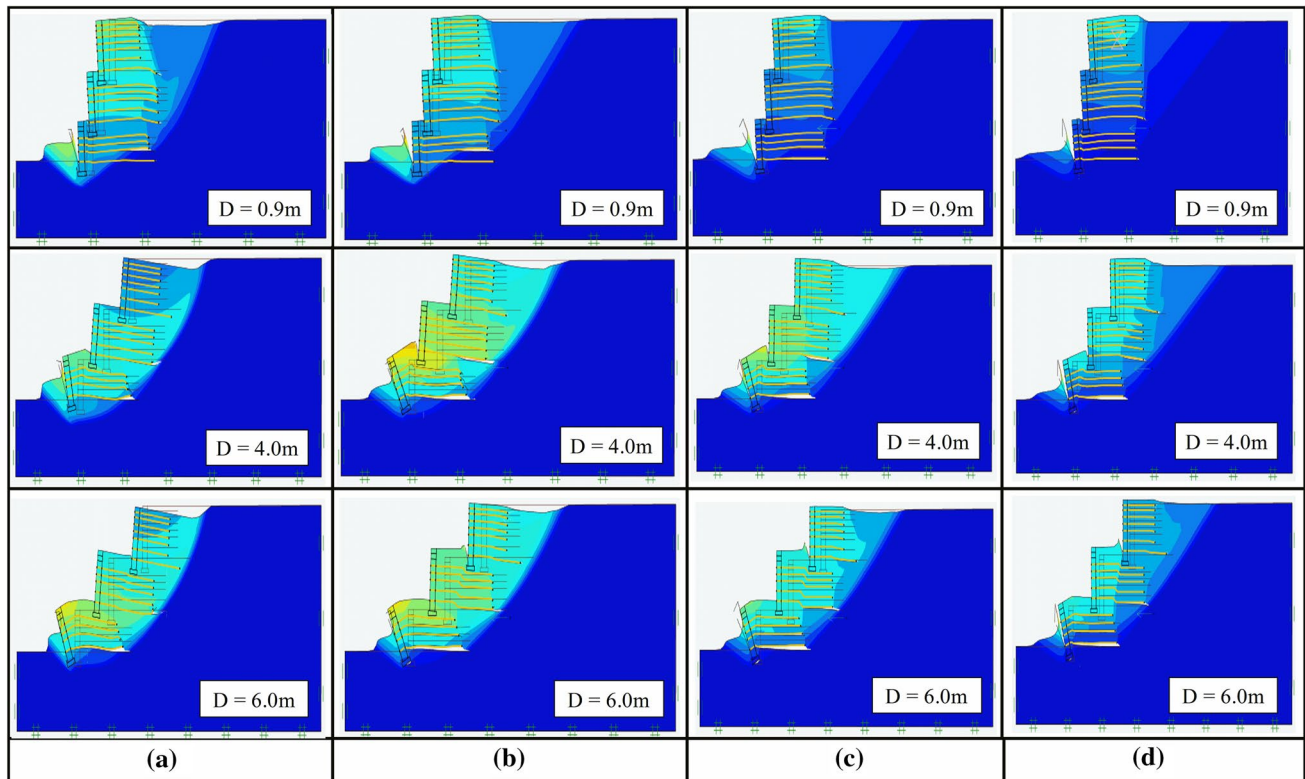


Fig. 11 The mode of failure for two-tiered MSE wall at **a** $k_h=0$; **b** $k_h=0.12$; **c** $k_h=0.24$; and **d** $k_h=0.36$

With an increase in the magnitude of k_h values, the sliding is reduced and the failure mode is purely overturning in nature.

The two-tiered and three-tiered wall system perceives a similar phenomenon in which at a lower magnitude of k_h , the wall experiences sliding and overturning failure both but with the increase in the k_h , it is observed that the failure mode is purely overturning. The offset distance also plays a significant role in the failure mode of the two-tiered wall as demonstrated in Figs. 10 and 11. For smaller offset distances, the soil mass in between the two interacting tiers is not affected at all, but as the offset distance (D) between two successive tiers increases, that soil mass participates in the progression of the wall failure, being the highest at $D=6$ m. Moreover, with an increase in the offset distance, the magnitude of overall wall sliding and overturning is greater than that witnessed at a lower magnitude of the offset distance. Moreover, for the single-tiered and multi-tiered wall systems, the critical plane of failure originates at the bottom junction of the vertical facing and the leveling pad, creating a severely stressed zone underneath the leveling pad. This specific behavior may be accredited to the fact that the overall reinforced soil mass acts as a single entity, which causes the entire enormous reinforced zone to shift horizontally away from the backfill. Here, in the two-tiered MSE walls, under static loading, a combined plane of failure passes underneath the walls and interacts at the ends of the

lowermost reinforcement layer, further dispersing toward the backfill surface. Under seismic loading conditions, a clear gap in the path of the failure plane is seen, again originating at the toe of the wall with a stress zone beneath it, barely touching the geosynthetics of the lower tier. The failure plane does not interact with the upper tier at all, and the upper tier of the wall behaves as a surcharge load to the lower wall and consequently increasing the stresses in the bottommost portions of the lower tier of the wall.

In the three-tiered walls, under static loading, the critical failure plane originates from the bottom end and transmits through the end of reinforcements of the second tier and further extends toward the backfill surface without interacting with the topmost tier at all and acting as a single entity. This also explains the maximum stress is caused on the geosynthetic layers of the middle tier and the shifting of the high-stress zone from the toe to the backfill to the rigid boundary in the three-tiered walls. Similar to the other cases discussed earlier, the failure plane does not interact with the topmost tier of the wall at all.

It is also witnessed that the earth mass underneath the offset distance does not overlap the failure path in case of a tiered MSE retaining wall when the offset distance is smaller; however, with an increase in the offset distance, this backfill mass gets disrupted as well and participates in the failure envelope, thus explaining the fact that after a

designed offset distance the walls employ no influence over each other. Also, in the rectangular MSE retaining wall, it is observed that an increase in the magnitude of the horizontal seismic acceleration coefficient causes disruption in the soil mass below the leveling pad instead of the soil mass reinforced in between the geosynthetics, which causes the leveling pad to sink in advance to any other failure occurring in the reinforced wall section.

Progression of the displacement vectors

The finite element simulation of the geotechnical problems facilitates looking into the displacement of each node with their actual magnitude and direction. This helps one to look into the actual displacement of such structure, which might not be possible in the small-scale or full-scale model testing. Such practices help to locate the positions, from where a failure in the structure propagates. In view of the above, the progression of the displacement vectors of the single-tiered wall, two-tiered wall, and three-tiered wall, under static and seismic loading, is compared and shown in Figs. 12, 13, and 14, respectively.

The displacement vectors of the rectangular MSE wall are clustered along with the failure wedge, on the modular block facing and at the end of the reinforcements, thus depicting the dislocation of these entities as the wall

begins to fail. As the k_h values are increased from 0 to 0.36, it is observed that the density of these displacement vectors reduces on the facing and the backfill, but is intensified on the reinforcing ends and below the leveling pad. This observation highlights the fact that under the high horizontal seismic acceleration, maximum force is exerted on the leveling pad and the reinforcements, which combats the failure of the wall.

The displacement vectors for the two-tiered wall system are illustrated in Fig. 13. As apparent from the figure, these vectors are bunched at the topmost facing blocks, beneath the leveling pad, behind the reinforcements, and on the failure wedge. It is worth noticing that since there are two failure wedges present for two-tiered walls, these vectors are positioned along with both failure wedges and can be distinguished. With an increase in the k_h value from 0 to 0.36, it is witnessed that the displacement vectors are concentrated more toward the lower reinforcing layers, thus explaining the highest affected sections of the MSE wall changes as the k_h is increased. The offset distance creates a noteworthy control on the position of the displacement vectors. With an increase in D , the reinforcing layers of the bottom tier suffer distortion, whereas when the D was considerably low, there was no disruption in the layers of the bottom tier of the wall. This can be correlated with the fact that when the offset distance is small, both the tiers act as a single entity, behaving as a

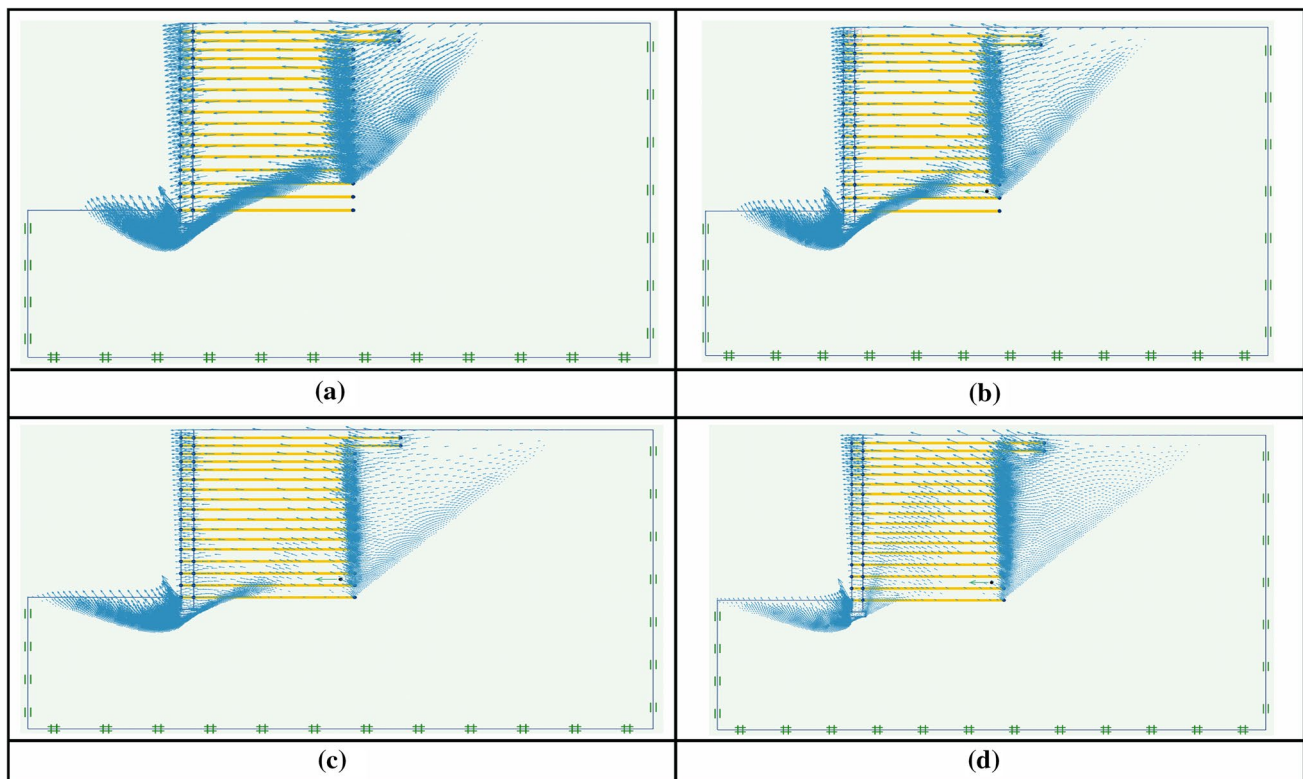


Fig. 12 The progression of displacement vectors for rectangular MSE wall at **a** $k_h=0$; **b** $k_h=0.12$; **c** $k_h=0.24$; and **d** $k_h=0.36$

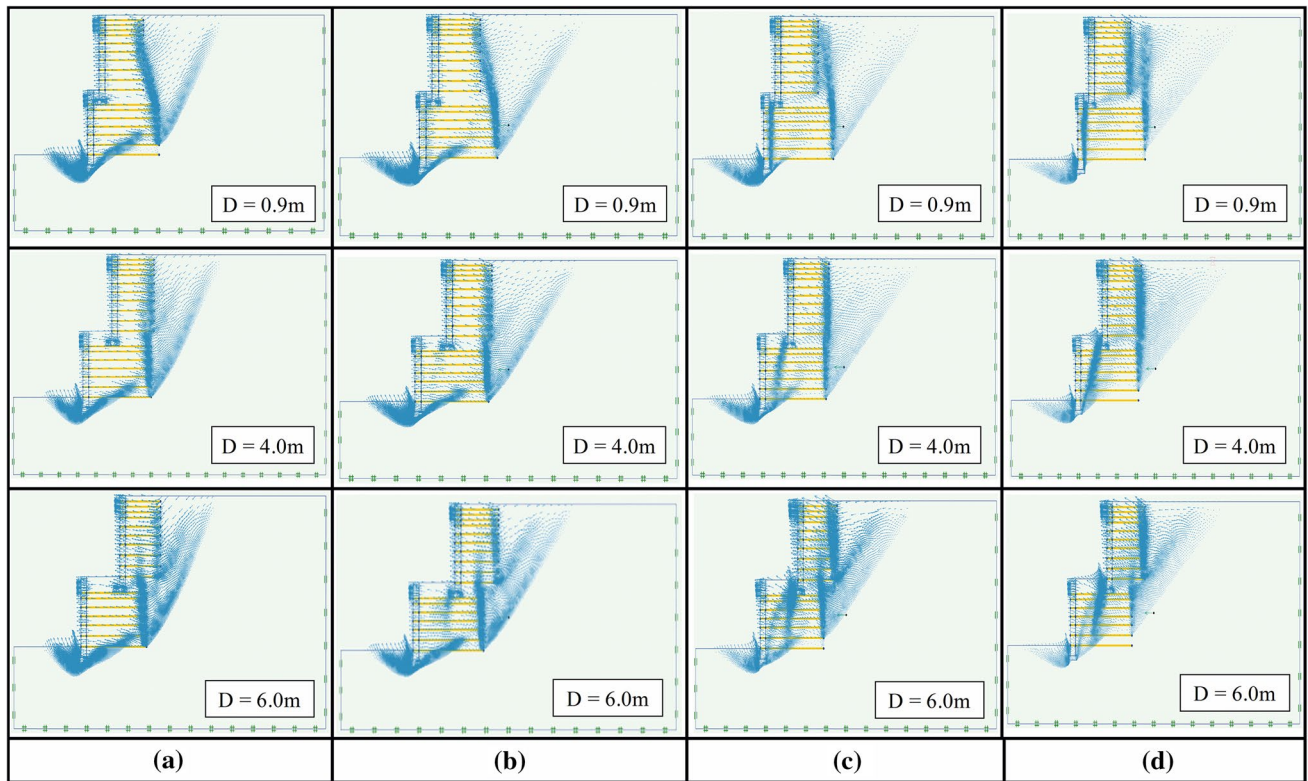


Fig. 13 The progression of displacement vectors for two-tiered MSE wall at **a** $k_h = 0$; **b** $k_h = 0.12$; **c** $k_h = 0.24$; and **d** $k_h = 0.36$

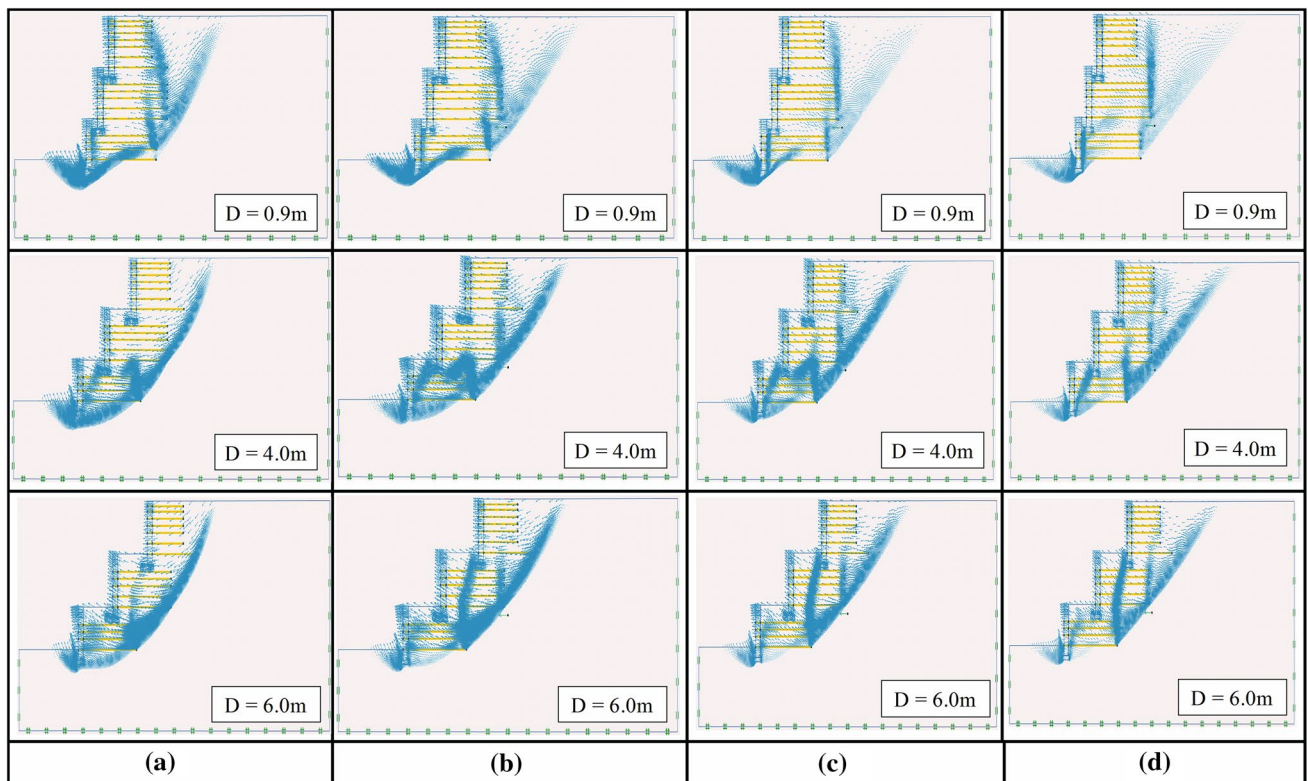


Fig. 14 The progression of displacement vectors for three-tiered MSE wall at **a** $k_h = 0$; **b** $k_h = 0.12$; **c** $k_h = 0.24$; and **d** $k_h = 0.36$

single wall. Hence, all the distortion of the wall is ensured by the upper layers of the reinforcement.

The displacement vectors of the three-tiered walls exhibit similar behavior as those experienced by the two-tiered walls. From Fig. 14, it is observed that as the offset distance increases, the position vectors along the failure wedge of the wall are more condensed, thus clarifying the effect of D on the three-tiered walls. Also, the reinforcing layers of the bottom tiers are highly influenced by both D and k_h . The increase in the horizontal seismic acceleration causes more effect on the leveling pad, reinforcing layers, and the facing rather than the backfill.

Effect on the factor of safety of tiered walls with the variation of the offset distance

With an increase in the offset distance, the effect exerted by the surcharge of the upper tiers on the lower one is reduced. However, when the offset distance is sufficiently increased, the surcharge effect is negligible and the wall behaves independently. Figure 15 illustrates the effect on the factor of safety (FOS) of the two-tiered and three-tiered wall system, w.r.t variation in D .

As per the guidelines laid by FHWA [13], FOS of 1.1 and above is acceptable for the MSE walls under seismic loading conditions. As evident from the graph, the FOS of the two-tiered and three-tiered walls at $k_h=0.12$ is more than sufficient to be feasible for seismic loading conditions. At $k_h=0.12$, on increasing the offset distance, the FOS of T_2D_2 increases by 5.2% than T_2D_1 , and the FOS of T_2D_3 increases by 2.9% than T_2D_2 . For T_3D_2 , a hike of 4% in FOS is observed than T_3D_1 .

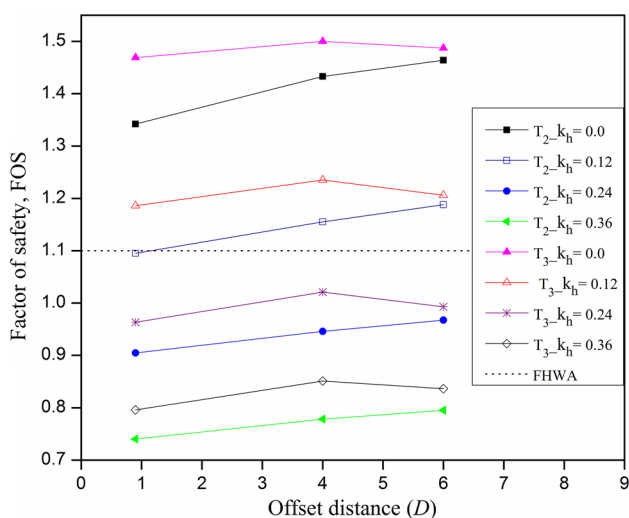


Fig. 15 Variation of the FOS w.r.t the offset distance for the two-tiered and three-tiered walls

Similarly at $k_h=0.24$, the FOS of T_2D_1 observes an increment of 4.6% than T_2D_1 and an increment of 2% when the FOS of T_2D_3 and T_2D_2 is compared with each other. In the case of comparison of T_3D_2 and T_3D_1 , a total hike of 6% is observed than the FOS of T_2D_3 increases by 2.9% than T_2D_2 .

Further, at $k_h=0.36$, a similar trend of the increment in FOS w.r.t increment in D is identified as well. The FOS increases by 5.1% and by 2.2% in between $T_2D_1-T_2D_2$ and $T_2D_2-T_2D_3$, respectively. Moreover, a surge of 6.9% is witnessed when the FOS of $T_3D_1-T_3D_2$ is compared. However, this study also notices a declination in the FOS of T_3D_3 on varying the k_h of the wall systems. Therefore, this study suggests that when the wall height is quite high, constructing a two-tiered wall with seismic loading consideration provides the best results.

Moreover, it is noticed that at high k_h at 0.24 and 0.36, the FOS of the tiered wall falls short than the FOS suggested by FHWA [13]. Since design guidelines presently available are ambiguous for multi-tiered walls under seismic loading conditions, it leaves a good scope for the researchers, to perform a thorough study and suggest concrete solutions. To meet the serviceability criteria for the two-tiered and three-tiered walls under higher values of k_h , this study suggests increasing the length of the reinforcement and the stiffness of the reinforcement. Also, the spacing in between the reinforcing layers can be reduced. Since the length, stiffness, and spacing can be easily monitored, modifying the aforementioned parameters can significantly improve the FOS of the walls.

Effect of the variation of horizontal seismic acceleration coefficient (k_h) on FOS

The rectangular and multi-tiered wall systems experience some substantial changes in FOS due to the variation in the horizontal seismic acceleration coefficient (k_h), which is represented in Fig. 16.

As recommended by FHWA [13], for a securely designed wall system, “a factor of safety against sliding of 1.5 is typical for non-seismic loads and a factor of safety of 1.1 is used for seismic loads (engineering judgment must still be applied as to the applicability of pseudo-static analyses and the acceptable factor of safety might be varied with the uncertainties involved in a particular analysis).” For the rectangular wall of 18 m high, on increasing the k_h from 0.0 to 0.36, the FOS of the wall system deteriorates by 49.4%, thus making it unserviceable under seismic loading conditions. For T_2D_1 , T_2D_2 , and T_2D_3 at $k_h=0$ and 0.12, the FOS of both the walls exceeds the values established by FHWA [13] and emerges as a better alternative than the rectangular wall. However, with further increase in seismic loading (k_h from 0.24 to 0.36), the FOS of T_2D_1 , T_2D_2 , and T_2D_3 declines by 18.3%, 17.7%, and 17.8%, respectively.

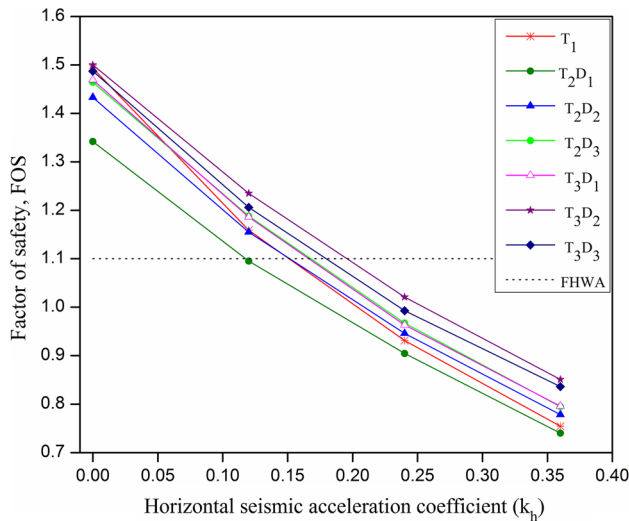


Fig. 16 Variation of the FOS w.r.t the horizontal seismic acceleration coefficient (k_h) for the two-tiered and three-tiered walls

The FOS of the three-tiered wall at different offset distances T_3D_1 , T_3D_2 , and T_3D_3 , increases as the k_h is increased from 0 to 0.24. At $k_h = 0.12$, the FOS of T_3D_1 and T_3D_2 and T_3D_3 is 7.8%, 12.2%, and 9.6% more than the FOS suggested by FHWA [13]. Hence, it can be proposed that if there occurs a necessity to construct a tall wall along with seismic loading circumstances, a tiered wall is a highly suitable alternative.

Again, it is perceived that at high k_h the FOS of the rectangular and tiered wall both falls below the FOS suggested by FHWA [13]. The present study suggests decreasing the spacing between the reinforcement and increasing the length of the reinforcement and the stiffness of the reinforcement to meet the serviceability criteria for the two-tiered and three-tiered walls under higher values of k_h .

Conclusions

The current study evaluates the stability of the MSE walls and their failure modes with the deviation of horizontal seismic acceleration coefficient k_h , offset distance D , in a single-heightened rectangular one, two-tiered, and three-tiered MSE wall system. From the results obtained, it is evident that all these parameters play a significant role in improving the overall stability of reinforced retaining walls of greater height. Also, this study presents an insight into the failure modes of the wall, where the rectangular, two-tiered, and three-tiered walls exhibit sliding and overturning failure both at a lower magnitude of k_h , but with the increase in the k_h , it is observed that the failure mode turns to purely overturning in nature. The factor of safety (FOS) values observed in this study are at par with the FOS suggested by FHWA [13], and

where they are not, this study suggests suitable measures to fulfill the respective serviceability criterion of these walls. The progression of the position vectors is also presented in-depth in this study, which states the influence of reinforcements, as they obstruct the overturning of the wall and assists in maintaining the stability of these walls. Furthermore, the critical wedge angle (β) is calculated for all the wall models. A wedge angle correction factor is introduced in this study to calculate the deviation of β from the β^* (critical wedge angle suggested by FHWA [13]), since there are no clear guidelines for multi-tiered walls under seismic loading conditions. These outcomes can be used as a reference for the further improvement in design manuals for high walls under seismic loading conditions.

Moreover, some characteristic conclusions obtained from the study are stated as follows:

1. From all the wall models simulated, the wedge angle obtained is not same as suggested by FHWA. Therefore, a wedge angle correction factor, C_Θ , is derived which is the ratio of the β^* obtained by the FHWA [13] guidelines and the β acquired for various wall models of the current study. It is noted that the wedge angle correction factor C_Θ for various walls under seismic loading ranges from 1.0 to 1.90 as given in Table 3. If the β^* suggested by FHWA shall be considered as the benchmark, then C_Θ helps in normalizing the deviation obtained in β derived for the rectangular, two-tiered, and three-tiered walls at varied k_h values.
2. The current study observes that at higher values of k_h specifically at $k_h \geq 0.24$, the obtained FOS of the multi-tiered walls, designed as per recommendations of FHWA [13], is not fulfilling the minimum required FOS values suggested by FHWA [13]. Therefore, to meet the serviceability criteria for the two-tiered and three-tiered walls under higher values of k_h , this study suggests increasing the reinforcement length compared to the recommended values by FHWA [13]. Alternatively, the spacing in between the reinforcing layers can also be reduced.
3. The rectangular and multi-tiered wall system experiences a combination of overturning and sliding failure. However, the sliding behavior reduces as the k_h increases, and the overturning failure is more prominent. For smaller offset distances, the soil mass in between the two interacting tiers is not affected at all, but as the offset distance increases, the soil mass participates in the progression of the wall failure, being highest at $D = 6$ m. Also, with an increase in the offset distance, the magnitude of wall sliding and overturning is greater than that witnessed at lower D . A triangular wedge shear failure formation is observed in both two-tiered and three-tiered MSE wall system where the critical failure plane of the

upper tiers combines with the failure plane of the lower tiers into a single failure plane propagating toward the horizontal backfill surface with a significant inclination with the vertical.

4. The FOS obtained for the two-tiered wall and the three-tiered wall is almost equal to the FOS obtained for the rectangular wall of similar height at the varied D and k_h . Thus, in regions where the land topography prohibits a deep excavation of 18 m, construction of tiered walls is a safe alternative as these walls need lesser excavation and are excellent in terms of serviceability as derived in this study.
5. It is evident that the two-tiered and three-tiered walls disperse the position vectors from the backfill and the failure wedge to the facing, reinforcing layers and soil mass beneath the leveling pad as the D and k_h increase, thus reducing the chances of the wall failure which is highly anticipated in case of rectangular walls. Since the quality of facing, reinforcements, and leveling pad can easily be controlled, rather than managing the quality of the backfill, it is feasible to build a safer wall in a tiered system rather than one single high rectangular wall. Hence, this study suggests building a tiered wall system instead of a rectangular wall.

Acknowledgements The first author acknowledges the support received from Mr. Sagar Jaiswal, PG Student, Civil Engineering Department, MMMUT Gorakhpur, UP, India, for the technical support for the finite element simulations using Optum G2.

Declarations

Conflict of interest The authors declare that they have no conflict of interest.

References

1. Dasaka SM, Dave TN, Gade VK, Chauhan VB (2014) Seismic earth pressure reduction on gravity retaining walls using EPS geo-foam. In: Proceedings of 8th international conference on physical modelling in geotechnical engineering, Perth, Australia, pp 1025–1030
2. Chauhan VB, Dasaka SM (2018) Performance of a rigid retaining wall with relief shelves. *J Perform Constr Facil* 32(3):04018021. [https://doi.org/10.1061/\(ASCE\)CF.1943-5509.0001161](https://doi.org/10.1061/(ASCE)CF.1943-5509.0001161)
3. Chauhan VB, Khan R, Dasaka SM (2019) Reduction of surcharge induced earth pressure on rigid non-yielding retaining wall using relief shelves. In: I.V. A, Maji V (eds) *Geotechnical applications. Lecture notes in civil engineering*, vol 13. Springer, Singapore, pp 209–217. https://doi.org/10.1007/978-981-13-0368-5_23
4. Sankey JE, Soliman A (2004) Tall wall mechanically stabilized earth applications. In: *Geotechnical engineering for transportation projects*, pp 2149–2158. [https://doi.org/10.1061/40744\(154\)211](https://doi.org/10.1061/40744(154)211)
5. Srivastava A, Jaiswal S, Chauhan VB (2021) Numerical study of geosynthetic-reinforced soil wall subjected to static footing loading. *Proc Eng Tech Innov* 17:13–20. <https://doi.org/10.46604/peti.2021.6693>
6. Bathurst RJ (2019) Developments in MSE wall research and design. In: *Innovative infrastructure solutions using geosynthetics, GeoMEast 2019, sustainable civil infrastructures*, pp 22–50. https://doi.org/10.1007/978-3-030-34242-5_3
7. Srivastava A, Chauhan VB (2020) Numerical studies on two-tiered MSE walls under seismic loading. *S N Appl Sci* 2(10):1–7. <https://doi.org/10.1007/s42452-020-03414-6>
8. Kongkitkul W, Tatsuoka F, Hirakawa D, Sugimoto T, Kawahata S, Ito M (2010) Time histories of tensile force in geogrid arranged in two full-scale high walls. *Geosynth Int* 17(1):12–32. <https://doi.org/10.1680/gein.2010.17.1.12>
9. Maheshwari P, Chauhan VB (2013) Beams on extensible geosynthetics and stone-column-improved soil. *Proc Inst Civ Eng Ground Improv* 166(4):233–247. <https://doi.org/10.1680/grim.12.00005>
10. Meyer ME, Woods CB, Axhushi N (2013) Reconstruction of a deteriorating, tiered, MSE wall structure in Connecticut. *International conference on case histories in geotechnical engineering*, vol 40, pp 1–7
11. Wilson P, Essery D, Taylor TP (2019) St. Jacques Pullman MSE walls lessons learned. In: *Transportation association of Canada and ITS Canada 2019 joint conference and exhibition*, pp 1–15
12. Wright GS (2005) *Design guidelines for multi-tiered MSE walls*. Austin, Texas, Report No. FHWA/TX05/0-4485-2, pp 1–118
13. Berg RR, Christopher BR, Samtani NC (2009) *Design and construction of mechanically stabilized earth walls and reinforced soil slopes*, vol I. Federal Highway Administration, Report No. FHWA-NHI-10-024
14. Leshchinsky D, Han J (2004) Geosynthetic reinforced multitiered walls. *J Geotech Geoenviron* 130(12):1225–1235. [https://doi.org/10.1061/\(ASCE\)1090-0241\(2004\)130:12\(1225\)](https://doi.org/10.1061/(ASCE)1090-0241(2004)130:12(1225))
15. Yoo C, Kim SB (2008) Performance of a two-tier geosynthetic reinforced segmental retaining wall under a surcharge load: Full-scale load test and 3D finite element analysis. *Geotext Geomembr* 26(6):460–472. <https://doi.org/10.1016/j.geotextmem.2008.05.008>
16. Liu H, Yang G, Ling HI (2014) Seismic response of multi-tiered reinforced soil retaining walls. *Soil Dyn Earthq Eng* 61:1–12. <https://doi.org/10.1016/j.soildyn.2014.01.012>
17. Bhattacharjee A, Amin MU (2019) Behaviour of two-tiered geosynthetic-reinforced soil walls. *INAE Lett* 4(2):91–100. <https://doi.org/10.1007/s41403-019-00069-7>
18. AASHTO LRFD (2004) *Bridge design specifications*, 3rd edn. American association of state highway and transportation officials, Washington, D.C.
19. Collin JG (ed) (1997) *Design manual for segmental retaining walls*, 2nd edn. National Concrete Masonry Association (NCMA)
20. Allen TM, Bathurst RJ (2019) Geosynthetic reinforcement stiffness characterization for MSE wall design. *Geosynth Int* 26(6):592–610. <https://doi.org/10.1680/jgein.19.00041>
21. Robert DJ (2017) A modified Mohr–Coulomb model to simulate the behavior of pipelines in unsaturated soils. *Comput Geotech* 91:146–160. <https://doi.org/10.1016/j.compgeo.2017.07.004>
22. Optum G2 (2020) *Finite element program for geotechnical analysis*. Optum Computational Engineering. www.optumce.com. Accessed 9 Apr 2021
23. Srivastava A, Jaiswal S, Chauhan VB (2020) The behavior of multi-tiered mechanically stabilized earth (MSE) retaining wall. In: *Proceedings of Indian geotechnical conference 2020, Visakhapatnam, India, Paper ID-TH-10-38*, 17–19 December 2020, pp 180–191
24. Jaiswal S, Srivastava A, Chauhan VB (2020) Performance of strip footing on sand bed reinforced with multilayer geotextile with wraparound ends. In: *Proceedings of Indian geotechnical*

- conference 2020, Visakhapatnam, India, Paper ID-TH-10-40, 17–19 December 2020, pp 192–202
25. Ojha R, Chauhan VB (2019) Performance of geosynthetic reinforced segmental retaining walls. In: Shehata H, Brandl H, Bouassida M, Sorour T (eds) Sustainable thoughts in ground improvement and soil stability GeoMEast 2019 sustainable civil infrastructures. Springer, Cham, pp 196–206. https://doi.org/10.1007/978-3-030-34184-8_13
 26. Portelinha FHM, Santos MC, Futai MM (2021) A laboratory device to evaluate geosynthetic load–strain behaviour in MSE walls. *Geosynth Int* 28(1):32–47. <https://doi.org/10.1680/jgein.20.00025>
 27. Holtz RD, Lee WF (2002) Internal stability analyses of geosynthetic reinforced retaining walls. Washington State Transportation Commission, No. WA-RD-532.1
 28. Jaiswal S, Chauhan VB (2021) Response of strip footing resting on earth bed reinforced with geotextile with wraparound ends using finite element analysis. *Innov Infrastruct Solut* 6:121. <https://doi.org/10.1007/s41062-021-00486-0>
 29. Kannaujiya P, Chauhan VB (2019) Behavior of anchored sheet pile wall. In: Shehata H, Brandl H, Bouassida M, Sorour T (eds) Sustainable thoughts in ground improvement and soil stability GeoMEast 2019 sustainable civil infrastructures. Springer, Cham, pp 184–195. https://doi.org/10.1007/978-3-030-34184-8_12
 30. Pandey A, Chauhan VB (2019) Numerical analysis for the evaluation of pull out capacity of helical anchors in sand. In: Shehata H, Brandl H, Bouassida M Sorour T (eds) Sustainable thoughts in ground improvement and soil stability GeoMEast 2019 sustainable civil infrastructures. Springer, Cham, pp 207–218. https://doi.org/10.1007/978-3-030-34184-8_14
 31. Jaiswal S, Srivastava A, Chauhan VB (2020) Numerical modeling of soil nailed slope using drucker-prager model. In: Proceedings of national conference on geo-science and geo-structures 2020, NIT Jamshedpur, India, Paper ID-GSGS020, 3–4 September 2020
 32. Ojha R, Srivastava A, Chauhan VB (2021) Study of geosynthetic reinforced retaining wall under various loading. In: Sitharam TG et al (eds) Ground improvement techniques: select proceedings of 7th ICRAGEE 2020, vol 118, pp 339–351. https://doi.org/10.1007/978-981-15-9988-0_31
 33. Xue JF, Chen JF (2015) Reinforcement strength reduction in FEM for mechanically stabilized earth structures. *J Cent South Univ* 22(7):2691–2698. <https://doi.org/10.1007/s11771-015-2799-9>